GASTROINTESTINAL

Hepatobiliary phase of gadoxetic acid–enhanced MRI in patients with HCC: prognostic features before resection, ablation, or TACE

Jae Seok Bae[1,2] · Jung Hoon Kim[1,2,3] · Dong Ho Lee[1,2] · Jae Hyun Kim[1,2] · Joon Koo Han[1,2,3]

Abstract

Objectives Patients with hepatocellular carcinoma (HCC) receiving different treatments might have specific prognostic factors that can be captured in the hepatobiliary phase (HBP) of gadoxetic acid–enhanced magnetic resonance imaging (GA-MRI). We aimed to identify the clinical findings and HBP features with prognostic value in patients with HCC.

Methods In this retrospective, single-institution study, we included patients with Barcelona Clinic Liver Cancer very early/early stage HCC who underwent GA-MRI before treatment. After performing propensity score matching, 183 patients received the following treatments: resection, radiofrequency ablation (RFA), and transarterial chemoembolization (TACE) ($n = 61$ for each). Cox regression models were used to identify clinical factors and HBP features associated with disease-free survival (DFS) and overall survival (OS).

Results In the resection group, large tumor size was associated with poor DFS (hazard ratio [HR] 4.159 per centimeter; 95% confidence interval [CI], 1.669–10.365) and poor OS (HR 8.498 per centimeter; 95% CI, 1.072–67.338). In the RFA group, satellite nodules on HBP images were associated with poor DFS (HR 5.037; 95% CI, 1.061–23.903) and poor OS (HR 9.398; 95% CI, 1.480–59.668). Peritumoral hypointensity on HBP images was also associated with poor OS (HR 13.062; 95% CI, 1.627–104.840). In addition, serum albumin levels and the prothrombin time-international normalized ratio were associated with DFS and/or OS. Finally, in the TACE group, no variables were associated with DFS/OS.

Conclusions Different HBP features and clinical factors were associated with DFS/OS among patients with HCC receiving different treatments.

Key Points

• *In patients who underwent resection for HCC, a large tumor size on HBP images was associated with poor disease-free survival and overall survival.*
• *In the RFA group, satellite nodules and peritumoral hypointensity on HBP images, along with decreased serum albumin levels and PT-INR, were associated with poor disease-free survival and/or overall survival.*
• *In the TACE group, no clinical or HBP imaging features were associated with disease-free survival or overall survival.*

Keywords Carcinoma, hepatocellular · Gadolinium DTPA · Magnetic resonance imaging · Treatment · Prognosis

Abbreviations

AFP	Alpha-fetoprotein
BCLC	Barcelona Clinic Liver Cancer

GA-MRI	Gadoxetic acid–enhanced magnetic resonance imaging
HBP	Hepatobiliary phase
HCC	Hepatocellular carcinoma
MVI	Microvascular invasion
PT-INR	Prothrombin time-international normalized ratio
RFA	Radiofrequency ablation
TACE	Transarterial chemoembolization

✉ Jung Hoon Kim
    jhkim2008@gmail.com

1 Department of Radiology, Seoul National University Hospital, 101 Daehak-ro, Jongno-gu, Seoul 03080, Republic of Korea

2 Department of Radiology, Seoul National University College of Medicine, 103 Daehak-ro, Jongno-gu, Seoul 03080, Republic of Korea

3 Department of Surgery, Seoul National University Hospital, 101 Daehak-ro, Jongno-gu, Seoul 03080, Republic of Korea

Introduction

Gadoxetic acid–enhanced magnetic resonance imaging (GA-MRI) is one of the primary imaging modalities for the

evaluation of patients with hepatocellular carcinoma (HCC) [1–3]. GA-MRI has been reported to have a higher sensitivity than extracellular contrast-enhanced MRI in the detection of HCC [4], probably because GA-MRI can detect additional nodules on hepatobiliary phase (HBP) images [5–7]. HBP images are obtained approximately 20 min after the injection of gadoxetic acid when maximal hepatic parenchymal enhancement is reached, according to the uptake of contrast media by normal, functioning hepatocytes [8]. Because pathologic lesions such as HCCs lack functional hepatocytes and do not uptake the contrast media and appear hypointense compared to surrounding hepatic parenchyma [9], HBP images provide excellent lesion-to-liver contrast that aids in the detection of such lesions. In addition to its diagnostic role, HBP images have been recently reported to have prognostic value for patients with HCC [10–12]. For instance, non-smooth tumor margins or peritumoral hypointensity on HBP images has been correlated with pathological microvascular invasion (MVI), which is associated with early recurrence after surgical resection or radiofrequency ablation (RFA) in patients with HCC [10, 13].

It can be hypothesized that there might be prognostic factors specific to patients with HCC receiving different treatments, and those factors may be captured in the HBP of GA-MRI. Obtaining prognostic information from as well as evaluating the presence or absence of HCC on HBP images may be clinically useful for choosing a treatment method and predicting the prognosis of patients with HCC [14]. For example, if there is an HBP feature that is specifically associated with poor prognosis after RFA, detecting that feature may lead physicians to consider alternatives such as resection or transplantation in that patient. The clinical impact of the prognostic value of HBP features might be enhanced by the increasing popularity of abbreviated GA-MRI protocols that rely on HBP images for the surveillance of HCC [15]. However, to the best of our knowledge, the prognostic value of HBP features for patients with HCC receiving different treatment methods has not been investigated.

Therefore, we aimed to identify the clinical findings and HBP features of GA-MRI with prognostic value in patients with HCC who underwent different treatments, including resection and locoregional therapy.

Materials and methods

This retrospective study was approved by the Institutional Review Board of Seoul National University Hospital (IRB No. 1901-036-1001), and the requirement for informed consent was waived.

Patients

We retrospectively included consecutive patients with HCC who underwent GA-MRI at Seoul National University

Hospital between January 2014 and December 2015. The inclusion criteria were as follows: (a) patients with HCC who met the non-invasive diagnostic criteria (i.e., arterial phase hyperenhancement and washout in the portal venous phase) [1, 2]; (b) patients with very early/early stage HCC according to the Barcelona Clinic Liver Cancer (BCLC) staging system [2]; and (c) patients with an interval between GA-MRI and treatment < 1 month. The exclusion criteria were as follows: (a) patients with HCC beyond the early stage; (b) patients who underwent treatment for HCC before the GA-MRI examination; (c) patients with a pathologic diagnosis after surgical resection that was not HCC; (d) patients who had other malignancies; and (e) patients who underwent liver transplantation or percutaneous ethanol injection after GA-MRI. We excluded patients who underwent transplantation or percutaneous ethanol injection because the numbers of those patients were relatively small ($n = 10$ and 9, respectively). Initially, 347 patients underwent the following treatments: resection ($n = 130$), RFA ($n = 96$), and transarterial chemoembolization (TACE) ($n = 121$) [16, 17]. Then, propensity score analysis using logistic regression and 1:1 matching among treatment groups was performed to reduce the effect of potential selection biases and confounding factors [18]. The variables used for propensity score matching were age, sex, etiology of liver disease, Child-Pugh score, serum alpha-fetoprotein (AFP) level, and tumor size and number on GA-MRI according to the radiologic reports. The final cohort comprised 183 patients with 183 HCCs ($n = 61$ for each treatment) (Fig. 1). Laboratory findings including the serum levels of albumin, total bilirubin, and AFP and prothrombin time-international normalized ratio (PT-INR) were gathered from the electronic medical records. For the patients who underwent resection, the presence or absence of MVI in the surgical specimens was recorded.
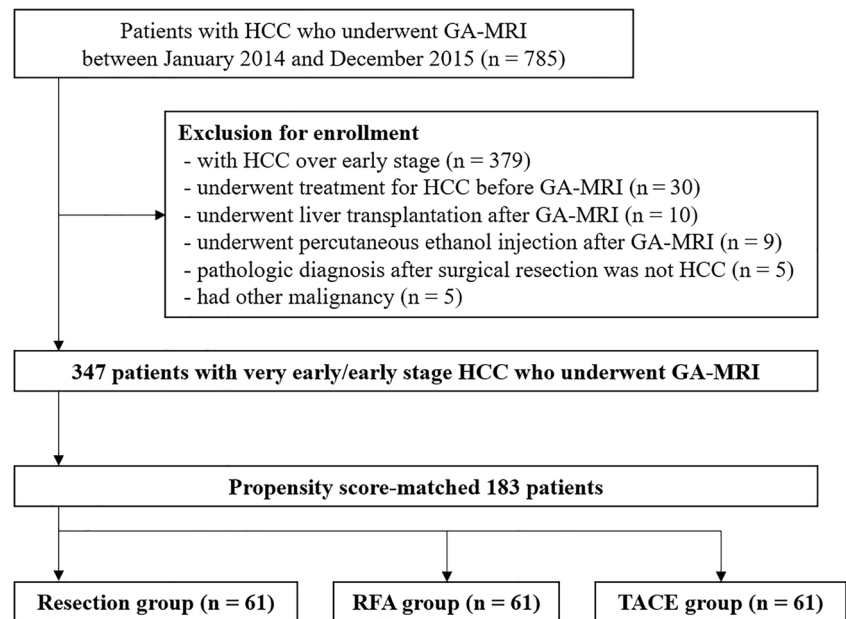
GA-MRI examination

GA-MRI was performed using either a 3.0-T or 1.5-T system. The liver GA-MRI protocol used in our institution included a breath-hold fat-saturated T2-weighted fast spin-echo or turbo spin-echo sequence, a three-dimensional T1-weighted dual-echo sequence, diffusion-weighted imaging, and dynamic three-dimensional fat-saturated T1-weighted gradient-echo sequences including HBP imaging. The details of our GA-MRI examinations are described in the Supplementary Material.

HBP image analysis

Two radiologists (D.H.L. and J.H.K., with 14 and 7 years of clinical experience in reading liver MRIs, respectively) who were informed that the patients had very early/early stage HCC but were blinded to the other clinical and pathological information independently evaluated the imaging features of

Fig. 1 Flow diagram of the study population. HCC hepatocellular carcinoma, GA-MRI gadoxetic acid–enhanced magnetic resonance imaging, RFA radiofrequency ablation, TACE transarterial chemoembolization

Patients with HCC who underwent GA-MRI between January 2014 and December 2015 (n = 785)

Exclusion for enrollment
- with HCC over early stage (n = 379)
- underwent treatment for HCC before GA-MRI (n = 30)
- underwent liver transplantation after GA-MRI (n = 10)
- underwent percutaneous ethanol injection after GA-MRI (n = 9)
- pathologic diagnosis after surgical resection was not HCC (n = 5)
- had other malignancy (n = 5)

347 patients with very early/early stage HCC who underwent GA-MRI

Propensity score-matched 183 patients

Resection group (n = 61) RFA group (n = 61) TACE group (n = 61)

HCC and liver function on HBP images. Although image analysis was performed only on HBP images, the radiologists could refer to any other pulse sequences to locate the HCC on the HBP images. The following HBP features of HCC were evaluated: number, size, signal intensity, heterogeneity, margin, capsule, peritumoral hypointensity, and satellite nodules. Tumor margins were graded as smooth or non-smooth [19]. The capsules were graded as absent, hypointense, or hyperintense [20]. Peritumoral hypointensity was defined as an irregular, wedge-shaped or flame-like hypointense area of liver parenchyma located outside of the tumor margin and was classified as absent or present [21]. Satellite nodules were defined as nodules < 1 cm in diameter outside the tumor margins within the venous drainage region, within 2 cm from the tumor, and were classified as absent or present [22]. To assess liver function, contrast between the liver and portal vein and biliary excretion into the common bile duct were evaluated [23, 24]. When there were multiple tumors, the largest tumor was assessed. Further details of the imaging feature analyses are described in the Supplementary Material. After independently reviewing the images, the two radiologists reached a consensus, and discrepancies were resolved through a discussion with another senior radiologist (J.H.K., with 22 years of clinical experience in reading liver MRIs).

Treatment and follow-up

The treatment method was chosen according to the European Association for the Study of the Liver guidelines for patients with very early/early stage HCC and included resection, RFA, or transplantation [2]. In our institution, however, TACE is frequently performed as a first-line treatment for patients who

cannot undergo RFA due to poor tumor visibility on ultrasound or a risky tumor location (i.e., abutting the hilar bile duct) [16, 17]. Because we excluded patients who underwent transplantation, our patients underwent one of the following three treatment methods: resection, RFA, and TACE. For each patient, the treatment method was chosen at the clinician's discretion considering age, general condition, and preference of the patient. Follow-up data after treatment were obtained by reviewing the electronic medical records of our institution and by accessing statistical data from the Korean Ministry of Government Administration and Home Affairs. Disease-free survival (DFS) and overall survival (OS) were defined as the interval between the date of treatment and the date of any kind of tumor progression or the date of death or last follow-up visit before July 31, 2019, respectively. The details of the follow-up protocol and assessments of recurrence are described in the Supplementary Material.

Statistical analysis

The baseline characteristics and HBP features of the patients were compared by using the chi-square test or Fisher's exact test for categorical variables and independent t test or the Mann-Whitney U test for continuous variables. Bonferroni correction was used for multiple pairwise comparisons. In the resection group, the associations between MVI and HBP features were assessed by using the chi-square test or Fisher's exact test. Linearly weighted kappa statistics and intraclass correlation coefficients were used to assess interobserver agreement for categorical and continuous variables, respectively. To interpret the interobserver agreement results, the following convention was used: < 0.20, poor; 0.21–0.40, fair; 0.41–0.60, moderate; 0.61–0.80, substantial; and 0.81–1.00,

Table 1 Clinical characteristics of study population

	Treatment			Total patients ($n = 183$)	p value*
	Resection ($n = 61$)	RFA ($n = 61$)	TACE ($n = 61$)		
Clinical feature					
Sex (male:female)	49:12	44:17	47:14	140:43	0.561
Age	59 (45–83)	60 (39–82)	63 (31–83)	60 (31–83)	0.074
Cause of underlying liver disease†					0.863
Chronic hepatitis B	51 (83.7)	48 (78.6)	47 (77.1)	146 (79.8)	
Chronic hepatitis C	6 (9.8)	5 (8.2)	6 (9.8)	17 (9.3)	
Alcoholic liver disease	3 (4.9)	4 (6.6)	5 (8.2)	12 (6.6)	
Others	1 (1.6)	4 (6.6)	3 (4.9)	8 (4.4)	
Laboratory finding					
Albumin (g/dL)	4.2 (2.8–4.9)	4.1 (2.9–4.9)	4.1 (2.9–4.9)	4.2 (2.8–4.9)	0.106
Total bilirubin (mg/dL)	0.7 (0.3–1.8)	0.7 (0.3–2.2)	0.7 (0.2–2.7)	0.7 (0.2–2.7)	0.287
PT-INR	1.06 (0.88–1.35)	1.08 (0.96–1.48)	1.07 (0.88–1.80)	1.07 (0.88–1.80)	0.100
AFP (ng/mL)	6.1 (1.1–2,193)	9.2 (1.4–4,660)	9.7 (1–23,810)	8.8 (1–23,810)	0.603
Child-Pugh score†					0.065
5	58 (95.1)	50 (82.0)	51 (83.6)	159 (86.9)	
6	3 (4.9)	11 (18.0)	10 (16.4)	24 (13.1)	

Except where indicated, data are median values with ranges in parentheses. *HCC* hepatocellular carcinoma, *PT-INR* prothrombin time-international normalized ratio, *AFP* alpha-fetoprotein, *RFA* radiofrequency ablation, *TACE* transarterial chemoembolization

*p value refers to the comparison among the patients in the resection group, RFA group, and TACE group

† Data are number of patients with percentages in parentheses

nearly perfect [25]. Survival curves were drawn by using the Kaplan-Meier method. Patients who underwent liver transplantation after the initial treatment were censored at the date of transplantation. The cumulative incidence of tumor recurrence was also calculated by using the Kaplan-Meier method. A univariable Cox proportional hazard model was used to reveal the clinical or HBP imaging features associated with OS and DFS. The variables with $p < 0.050$ were included in the multivariable Cox proportional hazard model. A p value < 0.050 indicated statistical significance. All

Table 2 Distribution of HBP features according to the treatment

	Treatment			Total patients ($n = 183$)	p value*	Interobserver agreement‡
	Resection ($n = 61$)	RFA ($n = 61$)	TACE ($n = 61$)			
Tumor size (cm), median (range)	2.5 (1–3.7)	2.1 (1–4.4)	1.7 (1–4.9)	2.1 (1–4.9)	0.116	0.954
Tumor signal intensity (hypo:iso:hyper)	59:2:0	57:3:1	59:1:1	175:6:2	0.727	0.657 (177/183)
Tumor heterogeneity (homogeneous:heterogeneous)	53:8	51:10	54:7	158:25	0.723	0.489 (161/183)
Tumor margin (smooth:non-smooth)	34:27	40:21	34:27	108:75	0.443	0.438 (130/183)
Tumor capsule (absent:hypo-:hyperintense)	56:4:1	56:5:0	60:0:1	172:9:2	0.210	0.682 (176/183)
Peritumoral hypointensity (absent:present)	51:10	56:5	54:7	161:22	0.375	0.574 (164/183)
Satellite nodule (absent:present)	58:3	59:2	60:1	178:5	0.596	0.347 (172/183)
Contrast between the liver and portal vein (iso-:slightly hyper-:hyperintense)	1:9:51	1:22:38	2:23:36	4:54:125	0.033†	0.173 (92/183)
Biliary excretion into the common bile duct (negative:minimal:moderate:complete)	3:4:15:39	4:6:11:40	8:6:18:29	15:16:44:108	0.317	0.358 (92/183)

HBP hepatobiliary phase, *RFA* radiofrequency ablation, *TACE* transarterial chemoembolization

*p value refers to the comparison among the patients in the resection group, RFA group, and TACE group

† Indicates $p < 0.05$

‡ Number in parentheses is the number of actual agreements divided by the total number

statistical analyses were performed using commercially available software (IBM SPSS Statistics for Windows, version 25, IBM; MedCalc, version 18.2.1).

## Results

Baseline characteristics of the patients

The baseline characteristics of the patients before and after propensity score matching are summarized in Table S2 and Table 1, respectively. Among these patients, 75 patients had very early stage HCC, and the remaining 108 patients had early stage HCC. The interval between GA-MRI and treatment was 11.8 ± 9.1 days (range, 0–31 days). In the resection group, MVI was observed in 18.0% (11 of 61 patients) of the surgical specimens. There were significant differences in DFS and OS among the three treatment groups.

HBP features according to different treatments

The HBP features are summarized in Table 2. The contrast between the liver and portal vein was relatively preserved in the resection group compared with that in the RFA or TACE group (isointense:slightly hyperintense:hyperintense, 1:9:51 vs. 1:22:38 vs. 2:23:36, $p = 0.033$). Otherwise, there was no significant difference in the distribution of HBP features among the treatment groups. In terms of MVI in the resection group, the tumors with MVI were significantly larger than those without MVI (median, 2.8 cm vs. 2.4 cm, $p = 0.042$). The other HBP features did not demonstrate differences regarding the presence of MVI ($p > 0.050$). Interobserver

Fig. 2 Representative images of patients without or with satellite nodules on hepatobiliary phase images. **a** This 61-year-old man had a 44-mm-sized hepatocellular carcinoma without satellite nodules. This patient did not experience recurrence for 50 months after radiofrequency ablation and was censored. **b** This 73-year-old man had a 42-mm-sized hepatocellular carcinoma but with a satellite nodule (arrow). Radiofrequency ablation was performed for this patient; however, intrahepatic distant recurrence was detected 12 months after treatment. **c** Kaplan-Meier curves demonstrated a significant difference in disease-free survival between patients without satellite nodules and those with satellite nodules ($p = 0.002$)
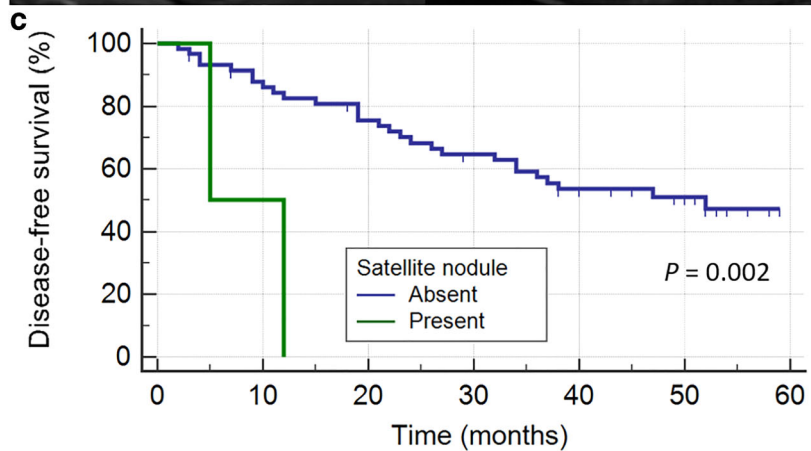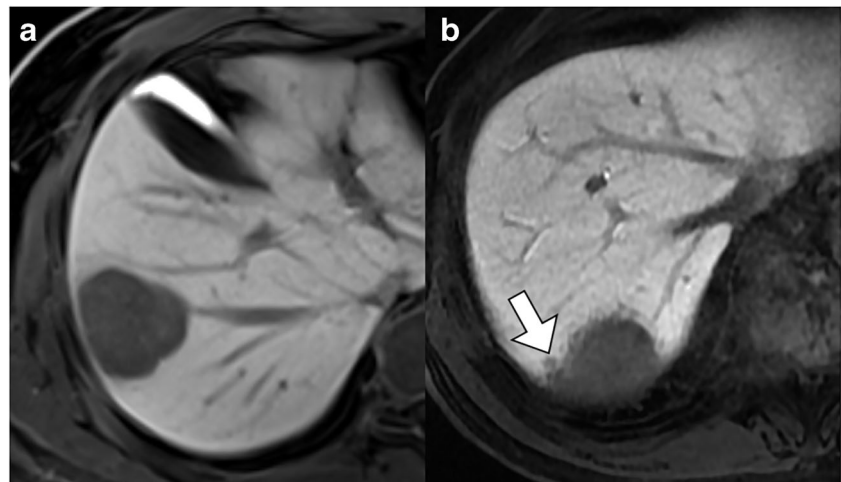
agreement for the HBP features ranged from poor to nearly perfect (0.173–0.951).

Clinical and HBP features with prognostic value for DFS in patients receiving different treatments

After receiving their treatments, the patients were followed up for a median (range) and mean ± standard deviation (SD) period of 51 months (5–66 months) and 47.3 ± 14.3 months, respectively. The median (range) and mean ± SD DFS were 32 months (2–65 months) and 31.0 ± 19.9 months, respectively. During surveillance after treatment, 14 patients were lost to follow-up. The estimated 1-, 3-, and 5-year DFS rates after treatment for HCC were 74.9%, 51.8%, and 40.0%, respectively. The patients in the resection group (47.7 months) and RFA group (39.0 months) had a better mean DFS than those in the TACE group (26.2 months) ($p < 0.001$ and $p = 0.001$, respectively), whereas there was no significant difference in mean DFS between the resection group and RFA group ($p = 0.124$). Of the 95 patients in whom recurrence was detected, local tumor progression developed in 25, intrahepatic distant recurrence developed in 68, and extrahepatic metastasis developed in 2. When assessed according to treatment group, recurrence (local tumor progression/intrahepatic distant recurrence/extrahepatic metastasis) occurred in 22 (1/20/1), 30 (4/26/0), and 43 (20/22/1) patients in the resection, RFA, and TACE groups, respectively. In terms of the results of the multivariable Cox proportional hazard model, in the resection group, tumor size (hazard ratio [HR] 4.159 per centimeter; 95% confidence interval [CI], 1.669–10.365) on HBP images was the only feature associated with DFS (Table S3). In the RFA group, serum albumin level (HR 0.390; 95% CI, 0.166–0.917) and satellite nodules on HBP images (HR 5.037; 95% CI, 1.061–23.903) were associated with DFS (Fig. 2) (Table S4). Finally, in the TACE group, no clinical factors or HBP features were significantly associated with DFS (Table S5).

Table 3 Clinical and HBP features of prognostic value for overall survival in the resection group

	Univariable analysis			Multivariable analysis		
	HR	95% CI	*p* value	HR	95% CI	*p* value
Female sex	1.046	0.117, 9.373	0.968			
Age	1.096	1.000, 1.200	0.049[†]	1.100	0.966, 1.251	0.150
Albumin (g/dL)	0.516	0.071, 3.760	0.514			
Total bilirubin (mg/dL)	0.153	0.003, 9.360	0.371			
PT-INR	4.314	0.000, 53940	0.761			
AFP (ng/mL)	1.001	0.997, 1.004	0.806			
Microvascular invasion in surgical specimen	1.274	0.142, 11.414	0.829			
HBP feature						
Tumor size	17.893	2.116, 151.323	0.008[†]	8.495	1.072, 67.338	0.043[†]
Tumor signal intensity						
Hypointense	< 0.001	6.1E−239, 11.4E+228	0.969			
Tumor heterogeneity	1.810	0.202, 16.219	0.596			
Tumor margin	5.668	0.633, 50.734	0.121			
Tumor capsule						
Isointense	< 0.001	8.1E−280, 100E+267	0.971			
Hyperintense	< 0.001	0.000, 10.1E+303	0.986			
Peritumoral hypointensity	< 0.001	5.0E−181, 126E+168	0.955			
Satellite nodule	15.137	2.510, 91.283	0.003[†]	6.161	0.760, 49.950	0.089
Contrast between the liver and portal vein						
Slight hyperintense	0.423	0.000, 10.1E+303	> 0.999			
Hyperintense	0.316	0.000, 10.1E+303	> 0.999			
Biliary excretion into the common bile duct						
Minimal	1.000	0.000, 10.1E+303	> 0.999			
Moderate	173622	0.000, 10.1E+303	0.974			
Marked	95917	0.000, 10.1E+303	0.976			

HBP hepatobiliary phase, *HR* hazard ratio, *CI* confidence interval, *PT-INR* prothrombin time-international normalized ratio, *AFP* alpha-fetoprotein.
[†] Indicates $p < 0.05$

Clinical and HBP features with prognostic value for OS in patients receiving different treatments

The estimated 1-, 3-, and 5-year OS rates after treatment for HCC were 98.4%, 85.8%, and 82.0%, respectively. During the follow-up period, 30 of the 183 patients (16.4%) died because of HCC progression ($n = 14$), liver failure ($n = 6$), variceal bleeding ($n = 2$), septic shock ($n = 2$), or an unknown cause ($n = 6$). Three of the 183 patients (1.6%) underwent liver transplantation for HCC recurrence after a median follow-up of 27 months (range, 13–58 months). There was no significant difference in mean OS among the treatment groups ($p = 0.062$).

In the resection group, a large tumor size on HBP images was associated with poor OS (HR 8.495 per centimeter; 95% CI, 1.072–67.338) (Table 3). In the RFA group, peritumoral hypointensity (HR 13.062; 95% CI, 1.627–104.840) and satellite nodules (HR 9.398; 95% CI, 1.480–59.668) on HBP images were associated with poor OS (Fig. 3) (Table 4). Serum albumin level (HR 0.064; 95% CI, 0.006–0.687) and PT-INR (HR 1413.55; 95% CI, 2.245–889885) were also associated with OS. In the TACE group, no clinical factors or HBP features were significantly associated with OS (Table 5).

Discussion

This study demonstrated that there were different clinical factors and HBP features of prognostic value specific to patients with HCC receiving different treatments. In the resection group, a large tumor size was associated with poor DFS/OS. In the RFA group, satellite nodules and/or peritumoral hypointensity on HBP images, decreased serum albumin levels, and/or elevated PT-INR were prognostic factors for poor DFS/OS. Finally, in the TACE group, no clinical factors or HBP features were significantly associated with DFS/OS.

Table 4 Clinical and HBP features of prognostic value for overall survival in the RFA group

	Univariable analysis			Multivariable analysis		
	HR	95% CI	p value	HR	95% CI	p value
Female sex	1.118	0.216, 5.774	0.895			
Age	1.094	0.996, 1.202	0.062			
Albumin (g/dL)	0.061	0.011, 0.335	0.001[†]	0.064	0.006, 0.687	0.023[†]
Total bilirubin (mg/dL)	3.254	0.859, 12.328	0.083			
PT-INR	2149.37	24.614, 187693	< 0.001[†]	1413.55	2.245, 889885	0.027[†]
AFP (ng/mL)	1.000	0.997, 1.002	0.725			
HBP feature						
Tumor size	1.770	0.753, 4.159	0.190			
Tumor signal intensity						
Isointense	< 0.001	1.1E−193, 6.2E+183	0.962			
Hyperintense	< 0.001	0.000, 10.1E+303	0.991			
Tumor heterogeneity	0.938	0.113, 7.784	0.953			
Tumor margin	2.583	0.578, 11.543	0.214			
Tumor capsule						
Hypointense	< 0.001	1.6E−254, 5.4E+243	0.968			
Peritumoral hypointensity	6.350	1.188, 33.950	0.031[†]	13.062	1.627, 104.840	0.016[†]
Satellite nodule	18.249	3.297, 100.997	0.001[†]	9.398	1.480, 59.668	0.018[†]
Contrast between the liver and portal vein						
Slight hyperintense	< 0.001	1.1E−167, 14.4E+153	0.938			
Hyperintense	< 0.001	1.1E−168, 1.4E+153	0.928			
Biliary excretion into the common bile duct						
Minimal	< 0.001	2.5E−194, 214E+180	0.953			
Moderate	0.212	0.019, 2.341	0.206			
Marked	0.212	0.039, 1.159	0.073			

HBP hepatobiliary phase, *RFA* radiofrequency ablation, *HR* hazard ratio, *CI* confidence interval, *PT-INR* prothrombin time-international normalized ratio, *AFP* alpha-fetoprotein

[†] Indicates $p < 0.05$

Table 5 Clinical and HBP features of prognostic value for overall survival in the TACE group

|	Univariable analysis			Multivariable analysis		
	HR	95% CI	p value	HR	95% CI	p value
Female sex	0.748	0.217, 2.585	0.647			
Age	1.038	0.989, 1.088	0.131			
Albumin (g/dL)	0.496	0.166, 1.476	0.207			
Total bilirubin (mg/dL)	0.840	0.288, 2.448	0.750			
PT-INR	0.161	0.004, 7.424	0.350			
AFP (ng/mL)	1.000	1.000, 1.000	0.061			
HBP feature						
Tumor size	1.311	0.869, 1.979	0.197			
Tumor signal intensity						
Isointense	< 0.001	1.5E−266, 6.2E+255	0.970			
Hyperintense	< 0.001	3.5E−283, 268E+270	0.972			
Tumor heterogeneity	1.636	0.473, 5.661	0.437			
Tumor margin	1.343	0.532, 3.389	0.533			
Tumor capsule						
Hyperintense	4.744	0.612, 36.782	0.136			
Peritumoral hypointensity	0.340	0.045, 2.563	0.295			
Satellite nodule	< 0.001	3.4E−173, 21.0E+162	0.957			
Contrast between the liver and portal vein						
Slight hyperintense	0.722	0.089, 5.889	0.761			
Hyperintense	0.572	0.073, 4.479	0.595			
Biliary excretion into the common bile duct						
Minimal	0.844	0.141, 5.065	0.853			
Moderate	0.397	0.080, 1.973	0.259			
Marked	0.858	0.236, 3.123	0.817			

HBP hepatobiliary phase, *TACE* transarterial chemoembolization, *HR* hazard ratio, *CI* confidence interval, *PT-INR* prothrombin time-international normalized ratio, *AFP* alpha-fetoprotein

These results may serve as a reference when making treatment decisions. For instance, either RFA or resection would be recommended for a very early stage single HCC < 2 cm according to the BCLC staging system. However, our results indicate that resection might be preferred over RFA in that patient to improve OS if peritumoral hypointensity is observed on the HBP images. The prognostic implication of HBP features may be associated with MVI, which is a well-known risk factor for early recurrence and/or poor OS in patients with HCC [26]. All the HBP features that demonstrated prognostic value for DFS/OS in our study (i.e., large tumor size, satellite nodules, and peritumoral hypointensity) have been reported to be associated with MVI [27]. Interestingly, different HBP features of MVI showed different associations with different treatment methods. For example, peritumoral hypointensity was associated with OS in the RFA group only but not in the resection group or TACE group, whereas large tumor size showed prognostic value in the resection group only. This finding raises the possibility that different MVI-associated HBP features might have different mechanisms by which they

appear on HBP images, which could have different therapeutic implications. Although there was no significant association between HBP features and MVI in this study, we speculate that the relatively small number of patients in the resection group (n = 61) who were pathologically confirmed to have MVI may be responsible for the statistical insignificance. Further studies are warranted to elucidate the mechanism and relationship between HBP features and MVI.

Other HBP features, including a non-smooth tumor margin, tumor encapsulation, and high/isointense signal in the tumor, did not demonstrate an association with DFS/OS in our study. Although a few studies advocated for the association of these HPB features with MVI or their prognostic role in patients with HCC [12, 28–30], controversy remains in the literature [31, 32]. Regarding tumor encapsulation, Kim et al reported that a hypointense rim around the tumor on HBP may not necessarily indicate a tumor capsule or pseudocapsule [32, 33]. In terms of tumor signal intensity, only a small proportion of our tumors showed iso- or hyperintensity on HBP images (4.4% [8/183]), and this small number may have resulted in

Fig. 3 Representative images of patients without or with peritumoral hypointensity on hepatobiliary phase images. **a** This 74-year-old man had a 20-mm-sized hepatocellular carcinoma without peritumoral intensity. This patient survived 46 months after radiofrequency ablation and was censored. **b** This 40-year-old woman also had an 18-mm hepatocellular carcinoma with peritumoral intensity (arrow). This patient died 25 months after radiofrequency ablation. **c** Kaplan-Meier curve demonstrated a significant difference in overall survival between patients without peritumoral intensity and those with peritumoral intensity ($p = 0.013$)
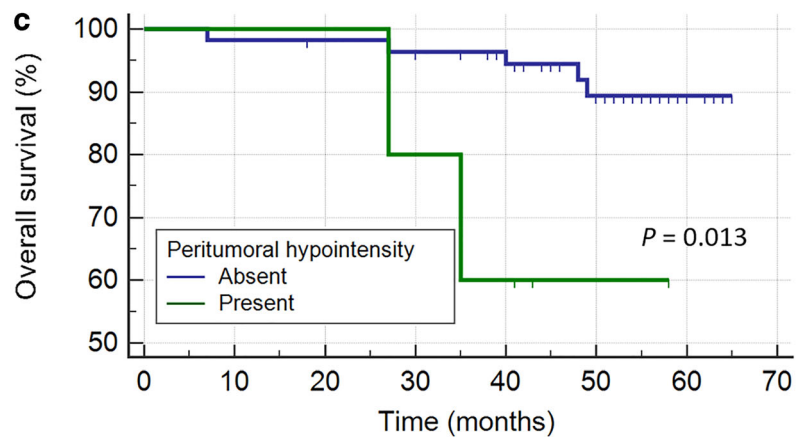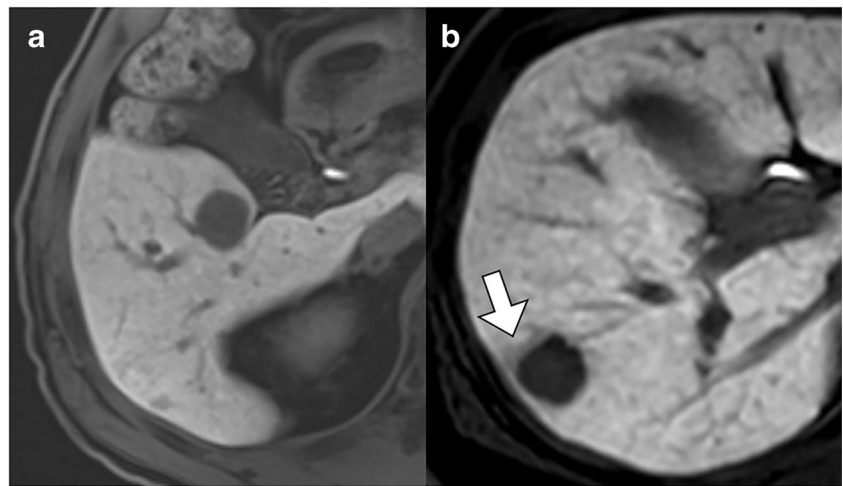
the lack of association between tumor signal intensity and prognosis.

There have been studies on the prognostic values of other pulse sequences of gadoxetic acid–enhanced MRI, such as enhancement patterns on dynamic T1-weighted images or diffusion-weighed imaging. In patients who underwent surgical resection for HCC, a low apparent diffusion coefficient map value has been reported to be associated with poor prognosis after resection [34, 35]. According to a recent study by Rhee et al, the arterial phase enhancement pattern is associated with macrotrabecular-massive HCC, which is a subtype of HCC that has a poor prognosis [36]. Other non-HBP imaging features, such as peripheral ragged enhancement, have been demonstrated to have prognostic value in patients who underwent TACE [37, 38].

In addition to the HBP features, a few clinical findings were also associated with DFS/OS in the RFA group: serum albumin level and PT-INR. Because both factors are associated with liver function [39, 40], the association of these laboratory results with DFS/OS in patients with HCC may reflect the importance of liver function. In the resection group and TACE group, however, no clinical findings or HBP features of liver function were associated with DFS/OS. One possible explanation for this result may be the inclusion criteria of this study: patients with preserved liver function (i.e., BCLC very early/early stage) were assessed. Moreover, propensity score matching for tumor number and size led to the selection of patients with single tumors and small HCCs. This selection criterion had a greater impact on the resection and TACE groups than on the RFA group because the resection group had larger tumors and the TACE group had more tumors than the RFA group before propensity score matching.

There were several limitations in this study. First, selection bias may have been present in our study because it is a single-center, retrospective study. In addition, there is a possibility that these HBP features might have affected treatment

decision-making, although there was no direct evidence that these HBP features were used to select the treatment method. However, we minimized this selection bias by including only treatment-naïve patients with very early/early stage HCC. Second, only HBP images were used, and information from dynamic studies, T2-weighted imaging, or diffusion-weighted imaging was not available. This situation may be problematic when diagnosing HCC. However, we focused on the prognostic role of HBP images, not on the diagnosis of HCC. Finally, an assessment of the association between MVI and HBP features was only possible in the resection group because the RFA and TACE groups lacked pathological information.

In conclusion, different HBP features and clinical factors were specifically associated with DFS/OS in patients with HCC receiving different treatment methods. The identified HBP features may have the potential to predict prognosis and select treatment methods for patients with HCC.

Compliance with ethical standards

References

1. Marrero JA, Kulik LM, Sirlin CB et al (2018) Diagnosis, staging, and management of hepatocellular carcinoma: 2018 practice guidance by the American Association for the Study of Liver Diseases. Hepatology 68:723–750

2. European Association for the Study of the Liver (2018) EASL clinical practice guidelines: management of hepatocellular carcinoma. J Hepatol 69:182–236

3. Korean Liver Cancer Association (KLCA); National Cancer Center (NCC), Goyang, Korea (2019) 2018 Korean Liver Cancer Association-National Cancer Center Korea practice guidelines for the management of hepatocellular carcinoma. Korean J Radiol 20:1042–1113

4. Roberts LR, Sirlin CB, Zaiem F et al (2018) Imaging for the diagnosis of hepatocellular carcinoma: a systematic review and meta-analysis. Hepatology 67:401–421

5. Ahn SS, Kim MJ, Lim JS, Hong HS, Chung YE, Choi JY (2010) Added value of gadoxetic acid-enhanced hepatobiliary phase MR imaging in the diagnosis of hepatocellular carcinoma. Radiology 255:459–466

6. Renzulli M, Biselli M, Brocchi S et al (2018) New hallmark of hepatocellular carcinoma, early hepatocellular carcinoma and high-grade dysplastic nodules on Gd-EOB-DTPA MRI in patients with cirrhosis: a new diagnostic algorithm. Gut 67:1674–1682

7. Kim YY, Park MS, Aljoqiman KS, Choi JY, Kim MJ (2019) Gadoxetic acid-enhanced magnetic resonance imaging: hepatocellular carcinoma and mimickers. Clin Mol Hepatol 25:223–233

8. Hamm B, Staks T, Muhler A et al (1995) Phase I clinical evaluation of Gd-EOB-DTPA as a hepatobiliary MR contrast agent: safety, pharmacokinetics, and MR imaging. Radiology 195:785–792

9. Huppertz A, Balzer T, Blakeborough A et al (2004) Improved detection of focal liver lesions at MR imaging: multicenter comparison of gadoxetic acid-enhanced MR images with intraoperative findings. Radiology 230:266–275

10. Lee S, Kim SH, Lee JE, Sinn DH, Park CK (2017) Preoperative gadoxetic acid-enhanced MRI for predicting microvascular invasion in patients with single hepatocellular carcinoma. J Hepatol 67:526–534

11. Ahn SJ, Kim JH, Park SJ, Kim ST, Han JK (2019) Hepatocellular carcinoma: preoperative gadoxetic acid-enhanced MR imaging can predict early recurrence after curative resection using image features and texture analysis. Abdom Radiol (NY) 44:539–548

12. Yamashita T, Kitao A, Matsui O et al (2014) Gd-EOB-DTPA-enhanced magnetic resonance imaging and alpha-fetoprotein predict prognosis of early-stage hepatocellular carcinoma. Hepatology 60:1674–1685

13. Lee S, Kang TW, Song KD et al (2019) Effect of microvascular invasion risk on early recurrence of hepatocellular carcinoma after surgery and radiofrequency ablation. Ann Surg. https://doi.org/10.1097/SLA.0000000000003268

14. Romanzi A, Ariizumi S, Kotera Y et al (2020) Hepatocellular carcinoma with a non-smooth tumor margin on hepatobiliary-phase gadoxetic acid disodium-enhanced magnetic resonance imaging. Is sectionectomy the suitable treatment? J Hepatobiliary Pancreat Sci. https://doi.org/10.1002/jhbp.743

15. Besa C, Lewis S, Pandharipande PV et al (2017) Hepatocellular carcinoma detection: diagnostic performance of a simulated abbreviated MRI protocol combining diffusion-weighted and T1-weighted imaging at the delayed phase post gadoxetic acid. Abdom Radiol (NY) 42:179–190

16. Teratani T, Yoshida H, Shiina S et al (2006) Radiofrequency ablation for hepatocellular carcinoma in so-called high-risk locations. Hepatology 43:1101–1108

17. Golfieri R, Cappelli A, Cucchetti A et al (2011) Efficacy of selective transarterial chemoembolization in inducing tumor necrosis in small (<5 cm) hepatocellular carcinomas. Hepatology 53:1580–1589

18. McDonald RJ, McDonald JS, Kallmes DF, Carter RE (2013) Behind the numbers: propensity score analysis-a primer for the diagnostic radiologist. Radiology 269:640–645

19. Ariizumi S, Kitagawa K, Kotera Y et al (2011) A non-smooth tumor margin in the hepatobiliary phase of gadoxetic acid disodium (Gd-EOB-DTPA)-enhanced magnetic resonance imaging predicts microscopic portal vein invasion, intrahepatic metastasis, and early recurrence after hepatectomy in patients with hepatocellular carcinoma. J Hepatobiliary Pancreat Sci 18:575–585

20. An C, Rhee H, Han K et al (2017) Added value of smooth hypointense rim in the hepatobiliary phase of gadoxetic acid-enhanced MRI in identifying tumour capsule and diagnosing hepatocellular carcinoma. Eur Radiol 27:2610–2618

21. Kim KA, Kim MJ, Jeon HM et al (2012) Prediction of microvascular invasion of hepatocellular carcinoma: usefulness of peritumoral hypointensity seen on gadoxetate disodium-enhanced hepatobiliary phase images. J Magn Reson Imaging 35:629–634

22. Choi JY, Lee JM, Sirlin CB (2014) CT and MR imaging diagnosis and staging of hepatocellular carcinoma: part II. Extracellular agents, hepatobiliary agents, and ancillary imaging features. Radiology 273:30–50

23. Tamada T, Ito K, Yamamoto A et al (2013) Simple Method for evaluating the degree of liver parenchymal enhancement in the hepatobiliary phase of gadoxetic acid-enhanced magnetic resonance imaging. J Magn Reson Imaging 37:1115–1121

24. Tamada T, Ito K, Sone T, Kanki A, Sato T, Higashi H (2011) Gd-EOB-DTPA enhanced MR imaging: evaluation of biliary and renal excretion in normal and cirrhotic livers. Eur J Radiol 80:e207–e211

25. Landis JR, Koch GG (1977) The measurement of observer agreement for categorical data. Biometrics 33:159–174

26. Chen SL, Xiao H, Xie ZL et al (2020) The presence of microvascular invasion guides treatment strategy in recurrent HBV-related HCC. Eur Radiol 30:3473–3485

27. Renzulli M, Brocchi S, Cucchetti A et al (2016) Can current preoperative imaging be used to detect microvascular invasion of hepatocellular carcinoma? Radiology 279:432–442

28. Lu DS, Siripongsakun S, Kyong Lee J et al (2013) Complete tumor encapsulation on magnetic resonance imaging: a potentially useful imaging biomarker for better survival in solitary large hepatocellular carcinoma. Liver Transpl 19:283–291

29. McHugh PP, Gilbert J, Vera S, Koch A, Ranjan D, Gedaly R (2010) Alpha-fetoprotein and tumour size are associated with microvascular invasion in explanted livers of patients undergoing transplantation with hepatocellular carcinoma. HPB (Oxford) 12:56–61

30. Kim JY, Kim MJ, Kim KA, Jeong HT, Park YN (2012) Hyperintense HCC on hepatobiliary phase images of gadoxetic acid-enhanced MRI: correlation with clinical and pathological features. Eur J Radiol 81:3877–3882

31. Zhang L, Yu X, Wei W et al (2020) Prediction of HCC microvascular invasion with gadobenate-enhanced MRI: correlation with pathology. Eur Radiol. https://doi.org/10.1007/s00330-020-06895-6

32. Lee S, Kim KW, Jeong WK et al (2020) Gadoxetic acid-enhanced MRI as a predictor of recurrence of HCC after liver transplantation. Eur Radiol 30:987–995

33. Kim B, Lee JH, Kim JK, Kim HJ, Kim YB, Lee D (2018) The capsule appearance of hepatocellular carcinoma in gadoxetic acid-enhanced MR imaging: correlation with pathology and dynamic CT. Medicine (Baltimore) 97:e11142

34. Lee S, Kim SH, Hwang JA, Lee JE, Ha SY (2019) Pre-operative ADC predicts early recurrence of HCC after curative resection. Eur Radiol 29:1003–1012

35. Muhi A, Ichikawa T, Motosugi U et al (2013) Diffusion-weighted imaging of hepatocellular carcinoma for predicting early recurrence and survival after hepatectomy. Hepatol Int 7:662–668

36. Rhee H, Cho ES, Nahm JH et al (2020) Gadoxetic acid-enhanced MRI of macrotrabecular-massive hepatocellular carcinoma and its prognostic implications. J Hepatol. https://doi.org/10.1016/j.jhep.2020.08.013

37. Kim BK, Kim KA, An C et al (2015) Prognostic role of magnetic resonance imaging vs. computed tomography for hepatocellular carcinoma undergoing chemoembolization. Liver Int 35:1722–1730

38. Park C, Kim JH, Kim PH et al (2020) Imaging predictors of survival in patients with single small hepatocellular carcinoma treated with transarterial chemoembolization. Korean J Radiol. https://doi.org/10.3348/kjr.2020.0325

39. Bellest L, Eschwège V, Poupon R, Chazouillères O, Robert A (2007) A modified international normalized ratio as an effective way of prothrombin time standardization in hepatology. Hepatology 46:528–534

40. Garcia-Martinez R, Caraceni P, Bernardi M, Gines P, Arroyo V, Jalan R (2013) Albumin: pathophysiologic basis of its role in the treatment of cirrhosis and its complications. Hepatology 58:1836–1846